Effect of Milling Frequency on the Structural and Dielectric Properties of Tetragonal Srtio$_3$ Nanoceramics

Iqra Irshad [1], Chaudhry Abu Bakar Imran [2]

[1] Centre of Excellence in Solid State Physics University of the Punjab, Lahore, Pakistan
[2] NUST Institute of Civil Engineering، School of Civil and Environmental Engineering، National University of Sciences and Technology, Islamabad, Pakistan
Corresponding author: Iqra Irshad,
Centre of Excellence in Solid State Physics, University of the Punjab Lahore, Pakistan
Email: iqrairshad166177@gmail.com

Abstract:

In this research work, we qualitatively study the structural and dielectric properties of tetragonal $SrTiO_3$ nanoceramics. The ferroelectric material with perovskite structure has various applications in different fields such as electronics and energy storage devices. Strontium titanate ($SrTiO_3$) among all ferroelectric materials has attractive attention due to its numerous applications as tunable microwave capacitor, thermistors, varistors sensors and microwave filters. Strontium titanate ($SrTiO_3$) nano-ceramics powders are prepared by solid state reaction route. Nano powders of strontium titanate are prepared by high energy planetary milling technique. The samples are prepared at various milling frequency of 15Hz- 50Hz for 4 h of milling time and then calcined at 1200 C for 60hrs. The calcined powders are characterized by XRD and Impedance analyzer. XRD studies reveal the p-cubic structure when the samples are milled at 15Hz to 35Hz of milling frequency and belong to space group of Pm3m. The phase transition from p-cubic to p-tetragonal was observed for the sample milled at 40Hz of milling frequency. After 40Hz of milling frequency no phase transitions in crystal structure of strontium titanate was observed. Only strengthening and phase stability of perovskite tetragonal $SrTiO_3$ was observed with increasing milling frequency. Dielectric and impedance analysis have been examined by impedance analyzer with a frequency range of 20Hz to 20MHz.Room temperature dielectric properties show immense dielectric constant value of ~ 73183.3 at 50Hz of milling frequency. The tangent loss is minimum for this sample. Colossal dielectric constant in nano-ceramics $SrTiO_3$ has impending applications such as in microelectronic devices as well as for the advancement of innovative capacitive data storage devices.

Keywords: Milling, Strontium Titanate, $SrTiO_3$ Nanoceramics, Composites, Electro Ceramic.

Introduction:

Strontium titanate ($SrTiO_3$) is remarkably interesting electro ceramic material because of its ferroelectric properties with heavy dielectric constant such as (300) on room temperature. Strontium titanate is useful in applications such as tunable microwave capacitors, Field emission display, as a diamond simulant, thermistors, and varistors. In addition at low temperature strontium titanate exhibit superconducting characteristics [2]. Dielectric properties depending upon temperature, frequency, particle size, density and material's composition and structure.

Thus to refine particle size is open is open question among the researchers. The dielectric properties alter with the processing conditions which are reported by several research groups. Many techniques can be applied for the production of nano sized STO powder such as ball milling, sol-gel, hydrothermal, sol-precipitation and organic polymeric [3].

The combination of two or more materials is called composites. Material from which the composite are made as separately substituents revealing the different chemical and physical properties. An extensive composite has been shown in figure 1. The examples of composites materials are plastic, polymer wood and metal alloy.

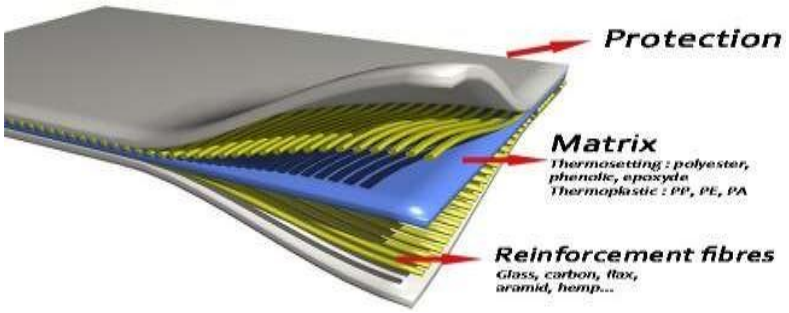

Figure 1: Composite materials [4]

Now days it is the demand to evolve such devices that are best quality, cheap and high rate of performance. Thus to obtain such characteristics we launch a material called composite material. Such properties which have to do with composites which are a) Cheaper b) Non corrosive c) Less in weight d) Electrical and thermal insulated, For example by using composite as a replacement of aluminum components we can decrease 20% - 50% weight.

Composites possess several key properties, including a high elastic modulus, low density, and resistance to corrosion, making them highly desirable for various applications. Due to these properties, composites are widely used in industries such as spacecraft and aircraft, marine and oil, as well as in bridge and building construction. Additionally, they are utilized in the production of consumer goods and automotive parts [5].

The mixture of metals called alloy i.e. when metallic elements are bound together in such a way that gold and copper, becomes red gold also gold and silver produce white gold. The very first alloy which was find is Bronze. Bronze contains 12-12.5% tin 85-88% copper and with the extension of other metal such as zinc, aluminum and nickel in small amount. Alloy are found to be harder, less ductile and more corrosion-resistant then the main metal as shown in figure 2.

Figure 2: Alloys

The mixture of alloy is stronger due to its different size of element from distinct atoms. A number of fusible alloys are prepared to melt at 90- 100 0C. Here are five alloying components such as a) chromium, b) molybdenum, c) Vanadium, d) Manganese e) Nickel. Now a day, alloy steels are the very significant alloy. It is defined as the steels which contains a number of elements except carbon and iron. The alloying elements for steel are nickel, silicon, manganese, tungsten and boron. The specific properties of alloys steel are such as corrosion resistance, hardness, ductility and magnetizibilty [6].

A solid material which is composed of metal, nonmetal which joins through ionic and covalent bond called a ceramic. Famous examples are porcelain, and brick. It became semi- crystalline and then change into totally amorphous when their crystal structure change for example lenses. When their crystals structure and bonds among electrons become change then make them super and good electric and thermal insulators. The ancient man-made ceramics were pottery items made either by humans or mix in flames with silica [9]. Some ceramics materials can see in figure 3. To avoid porous nature it was coated on ceramic substrate and for the purpose to get the soft and colored outlook. They are used in construction, art and industrial fields. Ceramic engineering had introduced in 20^{th} century.

Figure 3: Ceramic in different ways

During the research of solid-state chemistry scientist found different characteristics of structure of micro scales are related with properties of ceramics. 1/10 of angstrom (A^0) to 1/10 of micrometers is used to manufacture these materials. Microstructure contains grain boundaries, pores and many structural defects [10].Manufacturing technique and process conditions mostly indicating by microstructure. During the research of solid-state chemistry scientist found different characteristics of structure of micro scales are related with properties of ceramics. 1/10 of angstrom (A^0) to 1/10 of micrometers is used to manufacture these materials. Microstructure contains grain boundaries, pores and many structural defects [10]. Manufacturing technique and process conditions mostly indicating by microstructure.

They are essential in structural and construction field. For improvements in mechanical and work and their constituents the fracture mechanics is important instruments. By applying stress and strain to defects occurs in original substance the macroscopic collapse can be found. Fractography can be used to measure root of problem in substance. The ceramic bonds known as ionic and covalent can be characterize in amorphous and crystalline form .The material which is another form rather than any bond become the reason of fracture before plastic deformation that cause the poor toughness of materials. On the other hand the ductile metal failure modes when they combine leads to disastrous failure. To overcome this problem design a new field of ceramic products in which particular coating of ceramic fibers then embedded and fiber bridges are formed.

These methods nearly improve the tough nature of ceramics. Disk brakes are the use of ceramic with a particular method. When a ceramic is subjected to significant mechanical loading it undergoes an ice-tempting method. These methods are useful to control microstructure and also mechanical properties .when we use these methods power can be improve. To create macroscopic pores unidirectional arrangements that is allowed by ice-tempting [13]. The use of this oxides impose method are necessary in solid oxide fuel cells and filtration system of water.

Strontium

Strontium's discovered by William Cruickshank in 1787.It was named the Scottish town after where it was discovered. Alkaline is an earth metal which is great chemically reactive .When this is exposed into air, this metal's form a dark oxide layer, in periodic table calcium and barium. It primarily happens in strontium titanate minerals naturally. This is Mostly extracted from them.90 isotope is radioactive and it can be considered as atomic failure. On other side calcium is side natural stable strontium which is not harmful for health [14].Humphrey Davy first isolated strontium as a metal 1808 using the latest electrolysis method. Strontium naturally found only in compound with some other components, like strontium titanate and Celestine mineral's, because of oxygen and water having high reactivity. Prevent oxidation, we should place it with mineral oil or kerosene like liquid hydrocarbon, freshly expansion of strontium metal falsely form oxide of yellowish color which is shown in figure 1.2.Strontium metal containing five pyrophoric powder .Flames give a bright red color by volatile strontium salts and pyrotechnics and flares manufacture also use these salts .The raw strontium as show in figure 4.

Figure 4: Raw material of Strontium

In television cathode ray tubes made by strontium which can replaced by other display technologies Pyrotechnics and fireworks use strontium salts to obtaining a red color light (14).Radioactive isotopes of strontium have been used for some specific cancer treatment and in radioisotopes thermoelectric generators (RTGs) [15].

Titanium

Titanium with symbol Ti is a chemical element. From periodic table it is lie from group IV b with atomic number 22 and atomic mass number 47.86. Titanium is used in the form of alloy and it have low corrosion and high strength. Titanium and oxygen compound was exposed by William Gregory in 1791 [16]. Properties of Titanium are described in table 1.

Table 1: Element properties of Titanium

Element Properties	
atomic number	22
atomic weight	47.88
melting point	1,660 °C (3,020 °F)
boiling point	3,287 °C (5,949 °F)

Earth's crust constitutes 0.44 percent of titanium that is widely distributed .Is widely distributed. Totally rocks, clay, soils and sand are combined practically in this metal. It is also present in deep-sea dredging, stars plants, animals and natural waters [17]. The titanium metals are shown in following figure 5.

Figure 5: Titanium metal with High-purity (99.999 percent titanium metal).

The pure titanium is difficult to obtain due to its reactivity. After 1950 therefore special process has been invented that alters titanium to vital commercially formed structural metal from laboratory interest. The metallic titanium are formed by means of spongy in an electric arc the sponge may be fused. Extremely pure titanium on the labor tray scale can be made by vaporization the tetra iodide, $TiCl_4$ [18].

As titanium formed a surface film of inactive oxide therefore it has outstanding corrosion conflict. Its combinations of low density, high strength and outstanding corrosion conflict make it beneficial for spacecraft, ships, missile and aircraft. Titanium has also been promoted such as alloying accumulation in various steel to minimize the size and as a deoxidizer while to create hardening in copper [19].

Structure of Strontium Titanate (SrTiO3)

ABO3 exhibited perovskite structure. Strontium titanate is belonging to the perovskite family. This name to the structure is given by the $CaTiO_3$ mineral perovskite. In cubic the structure is a crude 3D square, with A-bigger cation at the corner and the oxygen anion in the focal point of the face edges, where A would be divalent trivalent and monovalent metal B - littler cation lie middle of the shape, where B would be a tetravalent, trivalent and pentavalent component. The existence of the octahedral BO6 is the very important characteristic of perovskite structure. The tetragonal and orthorhombic phases are very mutual non cubic modifications [20]. Here are a number of ABO_3 compounds which is distorted to lower symmetry from ideal cubic to tetragonal and orthorhombic etc. The perovskite crystal structure of cubic and tetragonal is shown in figure 6.

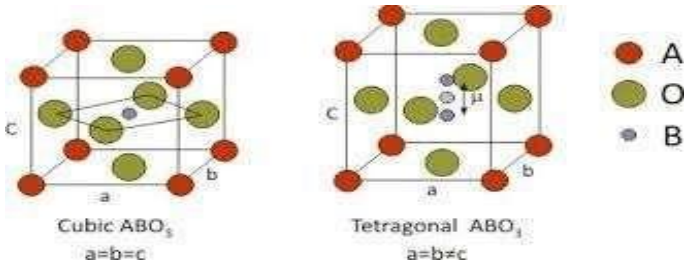

Figure 6: The perovskite crystal structure of cubic and tetragonal [21] Structural phase transition in strontium titanate

Strontium titanate with a perovskite structure ABO_3 at room temperature shows cubic structure. It has 0.3905 nm lattice parameter. The atomic structure is shown in figure 1.5. $SrTiO_3$ with mixed ionic- covalent bonding properties shows an exclusive structure, due to which it is known as an electronic materiel. At low temperature strontium titanate demonstrate nonlinear and tunable dielectric thin films that have a number of practical significance [22].

At room temperature (20 ^{0}C) and ~ -123.1^{0}C bulk STO shows cubic symmetry. This go through below this ~ -123.1^0 C a structural transition to a tetragonal phase. Tetragonal to orthorhombic structure at -208.15^{0}C was also recognized. ST obey curie Weiss law at T> - 223.15 ^{0} C [23]. For strontium titanate example shown below the Sr atoms occupy A site in the 12 coordinate while Ti sit in the 6 coordinate B site as shown in figure 7.

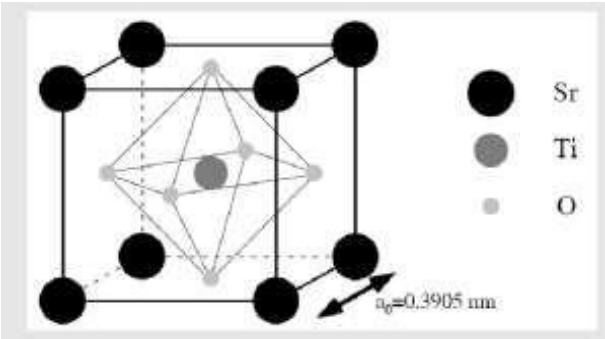

Figure 7: Atomic structure of $SrTi0_3$ at RT [24].

Table 2: Summary of the physical properties of $SrTiO_3$

Property	Value
Lattice parameter at RT (nm)	0.3905
Atomic density (g/cm^3)	5.12
Melting point (°C)	2080
Thermal conductivity (W/m·K)	12
Refractive index	2.31 - 2.38
Hardness	6
Dielectric constant (ε_0)	300

$SrTiO_3$ have perovskites structure. It is very alluring substances for the application to microelectronics as it have reliable insulating resources. A very excessive charge carrying capacity and magnificent optical transparency in the chemical balance. In past, $SrTiO_3$ was widely enroll in superconducting films because of lattice variable match [26]. Recently, in SrTio3 inspection purpose is to adjust the dielectric properties and optical properties. The increment of excessive dielectric permittivity of SrTiO3 at RT (~300) and between 100K to 240K. $SrTiO_3$ linked to low microwave losses. It makes it the highly advantageous substance for adjustable microwave electronic devices like that filters, oscillators, and delay lines, etc. When doped La, Nb,Ta vacancies[27]. The capability of srTion3 to switch conductivity is significant in the proposal of numerous electro ceramic apparatus for example capacitors, thermistors and varistors [28]. For unique uses in electronics, this is necessary to formulate mutually p-type and n-type $SrTiO_3$.

Though due to the compensation result caused by oxygen vacancies, p-type $SrTiO_3$ production is up to now little known and is scarcely produced. Though, p-type $SrTiO_3$ will be a very capable material. Firstly it is recognized that doping of p-type put up photonics conductivity in perovskite structures, secondly in blue-light region it would transform a wide-gap semiconductor diode and will be extremely appreciated in industry of semiconductor. Secondly the protonic conductors have wide range of electrochemical applications for instance hydrogen measuring device in industry of renewable energy- source and fuel cell [29]. Further technical uses of titanate-founded perovskites, such as $SrTiO_3$, involve their usage such as ceramic control of actinide and swarm phases for fission-product wastes. Actinide elements yield low energy heavy recoil nuclei as well as high energy alpha particles demanding the actinide excess to be there fused in appropriate matrices [30].

Dielectric and their Properties.

Electronic materials have extended so much significance because of their advancement in electronic devices such as materials can be categorized into conductors, insulators and semiconductor. Now the exclusive determination of this section is discussing dielectric properties of these materials. Dielectric properties are also examined by changing frequently and temperature for progressive application.

Dielectric

Dielectric is that kind of material that used to store charge and avoid flow of charge in electrical circuit. Dielectric be there usually considered insulator that gives the property of polarization. Dielectric properties can be defined by capacitor's capacitance. By placing dielectric to vacuum present among plates the ratio of capacitance is taken. The numerical measurement on dielectric was done by Faraday in 1837. Fundamentally dielectric is a Greek latter that means an insulating material [31]. It store charge in the presence of electric field by evolving polarization, thus there are present electric dipoles.

Electric dipole and Polarization (P)

Two equal but opposite charges which alter present a distance'd' known as electric dipole as shown in the figure. Resultant dipole moment designed by taking a product of charge and distance between them and its schematic diagram are shown in figure 8 and can be written as:

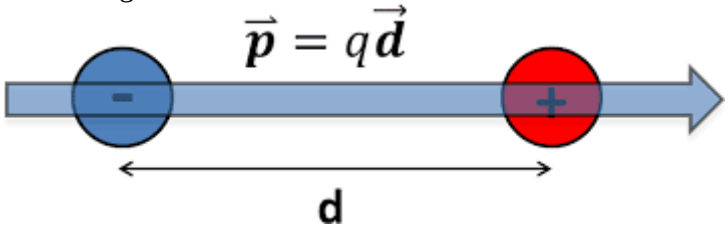

Figure 8: Electric dipole moment [32].

At extent, term polarization can also be distinct with the help of dipole moment definition. In the mechanism of polarization dipoles are develop where electric field are present. The net dipole moments per division volume is called the Polarization.

$P= Є \mu e / V$

Where V is the volume of overall sample .While all dipoles are bring into line in same direction at that time P written as Nm as shown in figure 1.5. Here N is number of dipole moments per division volume

c. Vector sum of dipoles are zero when P=0. Arrangement of dipoles in the presence of applied electric field is shown in figure 9.

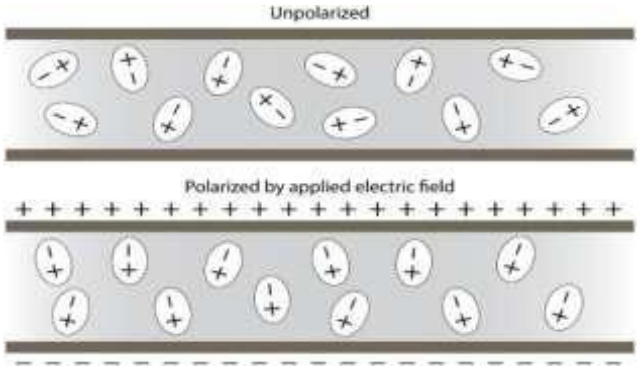

Figure 9: Arrangement of dipoles with applied electric field [33].

Polarization Mechanism

The material is electrically neutral as of the existence of positive and negative charges in the same amount. The charge neutrality can be concerned by functional electric field which provides the Polarization mechanism. Polarization mechanism has four types: a) Ionic polarization b) Electronic polarization c) Dipole polarization d) Space charge polarization [34]

Ionic polarization

Ionic polarization happens in materials that has ionic structure and contain cation and anions. While molecules share electrons in solid then electronic fog moves on the way to more electronegative atom .Hence observed there ionic polarization. These charges displace themselves from their equilibrium position at that time an external field applied, which is a result of net dipole moment. Ionic polarization occurs in 109 - 1013 Hz frequency range [35]. Electronic polarization

When an atom undergoes is applied electric field, Electronic polarization is observed. As nucleus have positive charge and electrons have negative charge, electronic cloud shifts towards one side and nucleus in the other side when an external field is applied and a displacement between them will happens which gives rise to the dipole moment such as polarization. Electronic polarization happens in the 1013-1015 Hz microwave frequency ranges. This kind of polarization can happen in almost all the type of non- conducting material so one can say that all the dielectrics are insulators.

Dipolar polarization

By sharing their valence electrons of two molecules dipolar material from a bond, which is the source of a dipole moment? Induced dipoles are randomly oriented hence the net polarization value is zero when there is no applied field. When field is given to these dipoles then it arrange in a line in definite direction which causes a dipolar polarization [36].

Space charge polarization

Interfacial polarization happens when charge build-up at the boundary of materials. In dielectric materials under ionic conduction this type of polarization arises as a result of the fact that the charges present in

these material that point towards the interface. This polarization creates a macroscopic field which is categories such as a bouncing polarization. Space charge polarization can be categories as hopping polarization and Interfacial polarization. Figure below shows the Polarization of these all four types in presence or without applied electric field. Influence of electric field on dipole is shown in figure 10.

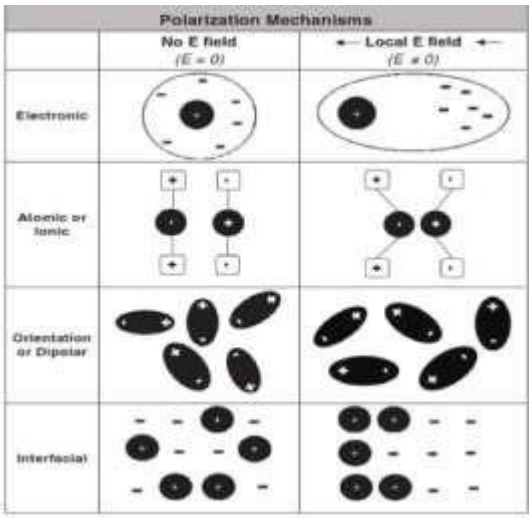

Figure 10: Types of polarization with and without applied electric field [37].

Frequency dependent polarization mechanism

When the external field is given to dielectric materials are polarized by dipoles rotate in the way of electric field. For this procedure to complete certain duration of time is required, which is changed for each polarization called the relaxation time. At the relaxation times the dipoles align themselves to way of electric field. While relaxation frequency of a given mechanism equals in frequency of given field then these results in maximum dielectric loss and energy is lost in form of heat .While if the applied frequencies higher than relaxation frequency the dipoles moment cannot reorient. So, the polarization mechanism does not contribute to the dielectric. Figure 11 below shows the frequency dependent different polarization mechanism of the dielectric material.

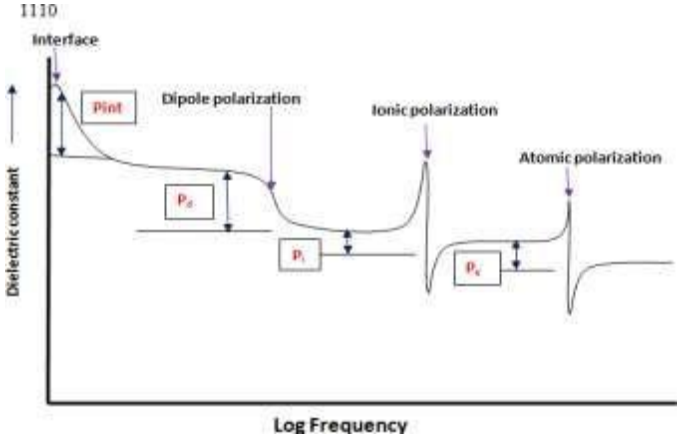

Figure 11: Polarization mechanism of frequency dependence

This Figure exhibit the variation of polarization with the frequency for dielectric materials which shows all four polarization mechanisms [38].

Types of Dielectric Materials

The dielectric material is categorized on origin of Polarization mechanism such as:

Linear Dielectric Material

The material which shows a linear relation between the applied field and polarization are called linear dielectrics. These materials become polarized when external electrical field is applied and become depolarized when field is removed. These materials are further categorized into 2 types due to the nature of Polarization;

a) Polar Dielectrics
b) Non- Polar dielectric [39]

Non-linear dielectric materials

Those materials that are natural polarized in the nonexistence of exterior electric field, these materials are known as nonlinear dielectric. This spontaneously polarization is due to the reason of the material's crystal structure. When the center of symmetry is absence then it leads to these materials to show this behavior. There are only 11 crystal have center of symmetry In the 32 crystal classes, and they don't show natural polarization. Whereas further 20 crystal sessions are piezoelectric 10 of these 20 classes, exhibit piezoelectric effect also temperature affect their polarization [40].

Dielectric Properties

In this chapter the dielectric properties of a dielectric material also discussed. The main dielectric properties contain dielectric loss, dielectric constant, and impedance spectroscopy etc.

Dielectric loss

Both imaginary and real parts are permittivity of dielectrics. When energy are loss of an AC signals when it passes over the dielectric is known as permittivity imaginary part of dielectric. It is symbolized by 'ε'. The dielectric constant and relative permittivity is known as real permittivity, which is denoted by Ɛ'. The relation between transmitted quickness of AC signal while capacitance of dielectric are described by real permittivity [41]. The dielectric loss is defined by the amount of the electric loss as heat by put on different electric field. The thesaurus of imaginary and real parts of permittivity with frequency is presented following in figure 12.

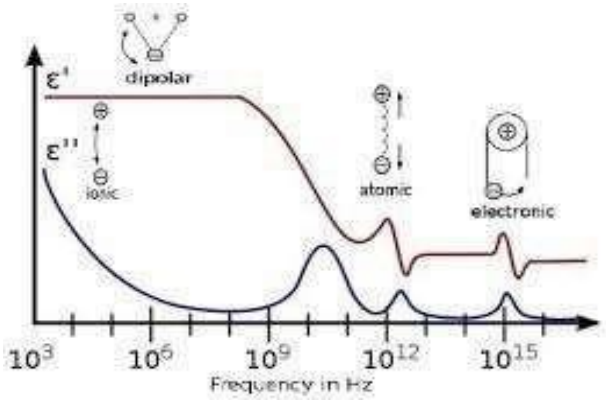

Figure 12: Ideal diagram for dielectric loss and dielectric constant

The imaginary part and real part are vertical to each other at entire time. The resultant dielectric constant is calculated by the sum of imaginary parts and real parts. The δ angle with real axis is created by resultant dielectric constant .The relation loss of material is proportion of energy lost and energy stored.

$$\tan \delta_{\varepsilon} = \frac{\varepsilon''}{\varepsilon'}$$

Where tan δ are known as tangent loss [42]. A quality factor Q is mentioned as:

$$Q = 1/ \tan \delta$$

Dielectric polymers and ceramics are insulators. A great dielectric constant with low dielectric loss are required for dielectric materials for capacitor high dielectric constant .Thus in some dielectrics such as strontium titanate ($SrTiO_3$, STO) the high dielectric constant are detected.

Dielectric constant

The aptitude of the material to electrical energy as applied electric field, it results into arrangement and separation of the charges. When these negative and positive charged separate, polarization is induced in the material .If the number of dipoles is higher and dipole moments and electric field are in same direction then the material show high permittivity. High dielectric materials are used as charge storage devices and capacitor Insulators are used as low dielectric materials.

Impendence Spectroscopy

The voltage V (t) in the time domain on applying signals low amplitude across a solid electrolyte, is defined as a complex impedance Z(Omega signs). To analyses the electrical response in the polycrystalline dielectric in a wide range of frequency is called impedance spectroscopy. The frequency dependence of impedance of a given circuit would form a semicircle in the complex plot between imaginary and the real parts of permittivity which demonstrate losses in capacitor [43-44]

Literature Review:

Y.Hu et al. [45] prepared nano- structure strontium titanate ($SrTiO_3$) at a low temperature dense film oxygen air instruments were achieved through ball milling method. The ball milling method is actual technique to fabrication of nano-scale powders of strontium titanate. $SrTiO_3$ nano-scale powders of about 20 nm remained manufactured after synthesis $SrTiO_3$ and commercial $SrTiO_3$. By using X-ray diffraction micro- structural material goods and oxygen sensing instrument material goods be there characterized. Investigational consequences demonstrate that recognizing properties were manufactured $SrTiO_3$ devices are much better with an strengthening temperature 400 ^{0}C rather than commercial $SrTiO_3$ devices. The recovery time with response time is 5 min and 1.6 min correspondingly. That is room temperature activated instruments. The identified variety is 1% oxygen to 20 % oxygen which is an extensive variety conceivable for a solitary type of material devices.

Y.Hu et al. [46] analyzed a stumpy temperature $SrTiO_3$ gas measuring device come to be invented by means of extreme –ball milling and conservative screen photogravure strategies. Grain size, thermal steadiness, lattice firm of fabric and detecting houses of measuring device tool at specific hardening temperature had been planned by using TEM, XRD, DTA and gasoline measuring device characterization correspondingly. The consequences display that hardening temperature effect simplest the particle length of manufactured nano-scale $SrTiO_3$ material that not transform perovskite structure. The eventual relative resistance rate of 6.35 gained for manufactured $SrTiO_3$ pattern annealed by 400 ^{0}C with working at 40 ^{0}C. The properties display that the exclusive annealing temperature most operational have an effect on the grain size of manufactured nano-scale $SrTiO_3$ material. The initial relative resistance price of 6.35 is usual for manufactured $SrTiO_3$ pattern which is annealing at 400 ^{0}C. The most useful working temperature such as the 40 ^{0}C is very lower rather than the conservative metal instruction oxygen gas measuring device.

Liu et al. [47] made up $Ba_{0.6}$ $Sr_{0.4}$ TiO_3 fine particles with in a ball milling technique. The handling parameters remained elevated on the way to attain ideal creation situation. BST nano-fine particle were imitative from precursor which is calcined at 1000 ^{0}C for 2 h. Then it is milled at 400/800 rpm for 5h. $Ba_{0.6}$

$Sr_{0.4}$ TiO_3 (BST) nano fine particle with negligible quantity of inferior segments can be resulting by HEBM treated precursors. By different milling process distinction of mean diameters and log normal dispersion of particle sizes obtained. The sample were milled at 400/800 rpm for 5 h. Then this sample was calcined at 1000 ^{0}C for 2h. At the end fine crystallized BST nano powders with mean grain size of 475 nm were developed.

Abdullah et al. [48] reported that dielectric material such as $SrTiO_3$ have significant attention. Nano-scale samples of $SrTiO_3$ were achieved by preparing it using the mechanical alloying method. The milled powder was sintered with numerous temperatures alternating from 500 ^{0}C to 1400 ^{0}C and pressed into pellets. XRD studied showed that at 900^{0}C these ceramics made a perovskite phase. SEM studies indicate the existence of small grain size from 120-600 nm extending. For sintering temperature 1000^{0}C to 1100^{0}C XRD peak data demonstrate vital increase in 'ε_r'. As sintering temperature increased from 500^{0}C to 1400 ^{0}C the dielectric constant at 1 MHz increases from 466 to 522.1 of sintered samples. By relating microstructural evolution characteristics and dielectric properties here are expansions in grain size thus imitating in a greater dielectric constant.

Babu et al. [49] manufactured the nano Strontium titanate perovskite structural ceramics powder have been via conservative solid state reaction method. ST precursor powder for nearly 20 h were ball milled and later for 9 h at 1000-1150 ^{0}C undergone calcinations and for 3h sintered at 1200^{0}C. The sample was characterized using XRD, EDX, TG-DTA, SEM and FTIR for structural, thermo gravimetric, microstructural and functional group analysis respectively. The properties such as dielectric constant 'ε_r' thermo electric power (S), dielectric loss (tan δ) and carrier concentration (η) be there calculated. The results showed that ε_r is decreasing with frequency and increasing with increase of temperature. To one side from this temperature (T) vs electrical conductivity (σ) was performed and the plot between ln T vs 1/T gives activation energies. The calculated values for dielectric constant are 136 at RT while 439 at 300 ^{0}C. $SrTiO_3$ achieved low dielectric loss and high dielectric constant thus useful in capacitors. Therefore $SrTiO_3$ became choosy material for applications in numerous systems such tunable capacitors and microwave device components.

Chowdhury et al. [50] considering Barium strontium titanate due to its important applications as the piezoelectric material in the electronic gadget. By high mechanical ball processing barium strontium titanate nano crystalline have been integrated from mechanical alloying of $SrCO_3$, $BaCO_3$ and TiO_2. By processing XRD, FESEM and DC electrometer the refined powders are described different phases. By XRD examination concluded that at 1200 ^{0}C barium carbonate slowly changed into barium strontium carbonate and then lastly into barium strontium titanate. Thus this supplementary change lessens the dielectric conduct of barium strontium titanate. From all this it was seen that capacitance from 20.47 pF to 3.06pF decreased. Thus a nano organized SBT having a orthorhombic and cubic shaped was organized.

Muraleedharan et al. [51] proposed that through solid state reaction technique via ball milling monitored $Ba_3SrTa_2O_9$ perovskite was synthesized. In this essay the result of the milling time discussed conductivity, morphological and structural properties. Due to taking a great amount of milling time the precursors' particle size are lesser that give rise to to lesser balance temperature which are investigated by thermo gravimetric analysis. After varied milling times of calcined samples, XRD data showed not at all variation in crystal structure. Due to lengthier milling time SEM pictures indicated degeneration of nano-crystallite. Solitary crystalline peeling morphology of atoms is showing by TEM images. $Ba_3SrTa_2O_9$ sample achieved subsequently 5 h milling showed a little well conductivity as matched to individuals samples attained afterwards 20 h milling that are exposed by electrical impedance analysis.

Kavitha et al. [52] reported that from solid state reaction technique, to gaining the procedure of only one phase perovskite is condensed through ball milling which is monitored from calcination. Thus production process formed only one crystalline perovskite that are in the arrangement of flakes are exposed by morphological and structural studies. When perovskite for shorter and longer duration are compared then the perovskite displayed improved electrical properties acquired afterward ball milling

intended for smaller time. Elongated ball milling time declines the properties of the perovkite Ba_3 Sr Ta_2 O_9 when manufactured via solid state reaction route.

Priyadharsini et al. [53] As dopant on the structural, morphological, and capacitance actions of SrTiO3 for super capacitor presentation this object is offering the result of the nickel. Untainted and Ni-dopedSrTiO3 was manufacture via ball milling method. By powder X-ray spreading (XRD) the stage construction and transparency of manufacturing models were completed. The character of dopants in setting the particle extent of SrTiO3 is displayed by the apparent morphology. The electrochemical presentation of uncontaminated and Ni-doped SrTiO3 was explored using cyclic voltammetry (CV)and Galvanostatic charge discharge(GCD)ina3-MKOHelectrolytesolution.It was originate that Ni- doped SrTiO3 showed the all-out precise capacity of 142 F/g at 1 A/g, which was meaningfully higher than that of uncontaminated SrTiO3 (105 F/g at 1 A/g). There is the smallest charge transference opposition charge for Ni-doped SrTiO 3 that model electrochemical impedance spectroscopy (EIS) demonstrate.

Pan et al. [54] To convince controllable differences in constructions and dielectric behaviors in oxides the limitation industrial concrete is used. By manifold ions (Nb, Zn)x+ (x=2, 3, 4 and 5) SrTiO3 ceramics modified by ordinary solid formal method adjustable valance condition are ready . By the methodically Phase structures, microstructures, deficiency structures and dielectric possessions of the (Nb, Zn) co-doped SrTiO3 ceramics have been examined. In acceptor co-doping, M2 ceramics (x=2) exhibits extremely low dielectric loss (≤0.001). M3 ceramics (x=3) shows low conductivity and excellent thermal stability. In corresponding co-doping, M4 ceramics (x=4) possesses oversize permittivity and low-slung dielectric damage. In , M5 ceramics (x=5) presents better-quality permittivity in donor co-doping while declined dielectric damage. The oxygen situation is beneficial to the localization of responsibility transporters and then the low-slung refraction loss, by the additional inquiries expose ,while additional electrons not only donate to the better-quality permittivity but similarly consequence in extraordinary dielectric damage .For the construction of numerous imperfection dipoles or shortcoming bunches are suitable concentration of oxygen position and electron , and consequently the significantly modified dielectric possessions. To cause the progressive electronic resources the findings might simplify the aptitude suitable

Rocha-Rangel et al. [55] prepared the strontium titanate samples, for which $SrCO_3$ and TiO_2 powders mixture are used. In a planetary mill raw material were started automatically. At different temperatures the raw materials calcined. In contrast samples resultant from heat treatment was characterized by XRD, electrical measurement and SEM. XRD examination governs those $SrTiO_3$ synthetized offerings the cubic structure of perovskite. A reaction for $SrTiO_3$ compound formation completed at 1200 ^{0}C. SEM remarks show the occurrence of a microstructure with very small grain size and thus huge number of grain boundaries. Firstly heating at 1000 or 1100^{0}C the original powder mixture was found, offerings the characteristics of strongly insulating material which is formed by $SrTiO_3$ .By heating the original powder mixture at 1200 or 1300 ^{0}C the other material with the cubic crystalline structure of the $SrTiO_3$ perovskite was attained. Due to their very low dielectric constants these materials have semi conductive characteristics.

Material & Methodology:

Electronic Weight Balance*:*

Used for precise material measurements, with an accuracy up to 0.0001g, and capable of measuring in different units (grams, pounds, etc.).

***Ball Milling**:*

SrTiO3 samples were prepared via high-energy ball milling (Model FRITSCH Pulverisette 23) using a 1:1 ratio of powder to ball. The milling process generates fine powders suitable for further analysis.

***Hydraulic Press**:*

Used to apply 30kN pressure to compact the powders into disk-shaped pellets.

***Nabertherm Furnace**:*

Employed for heat treatment by calcining pellets at 1200°C for 60 hours to develop their best form for analysis.

Sample Preparation

SrTiO3 was synthesized via solid-state reaction using ball milling. SrO and TiO2 powders were mixed, and the resulting mixture was ball-milled, then pressed into pellets and calcined at 1200°C. This cost-effective method produces nanoparticles at room temperature.

Characterization Techniques

***X-ray Diffraction (XRD)**:*

Used to determine the crystal structure and size of the SrTiO3 samples.

***Impedance Spectroscopy**:*

Measured dielectric properties, including dielectric constant, AC conductivity, and dielectric loss at various frequencies using a precision impedance analyzer (WAYNE-Kerr 6500B series, 20Hz to 20MHz).

Results and Discussion:

$SrTiO_3$ samples were prepared by solid state reaction method employing nano ball milling technique. The powders were milled at different milling frequency of 15Hz, 20Hz, 25Hz, 30Hz, 35Hz, 40Hz, 45Hz and 50 Hz and then calcined at 1200□C for 60hrs. To evaluate the properties of these samples, different techniques were used. X-ray diffraction (XRD) technique was used for the structural analysis. Dielectric properties were analyzed by Impedance Analyzer. Results for all the techniques are discussed below in detail.

Structural Analysis

The XRD patterns of strontium titanate nano-ceramics samples prepared by the Solid State Reaction method utilizing nano ball milling technique, unmilled and milled at different milling frequency of 15Hz, 20Hz, 25Hz, 30Hz, 35Hz, 40Hz, 45Hz and 50 Hz and then calcined at 1200 C for 60hrs are shown in Figure 13. The xrd patterns of unmilled and milled at 15Hz to 35Hz milling frequency exhibit cubic perovskite structure and belongs to space group of Pm3m. According to the JCPDs (PDF-01-089-4934) card, the recorded peaks of unmilled and milled at 15Hz to 35Hz milling frequency of $SrTiO_3$ are well indexed. The phase transition from p-cubic to p-tetragonal was observed for the sample milled at 40Hz of milling frequency. After 40Hz of milling frequency no phase transitions in crystal structure of strontium titanate was observed. Only strengthening and phase stability of perovskite tetragonal $SrTiO_3$ was observed with increasing milling frequency

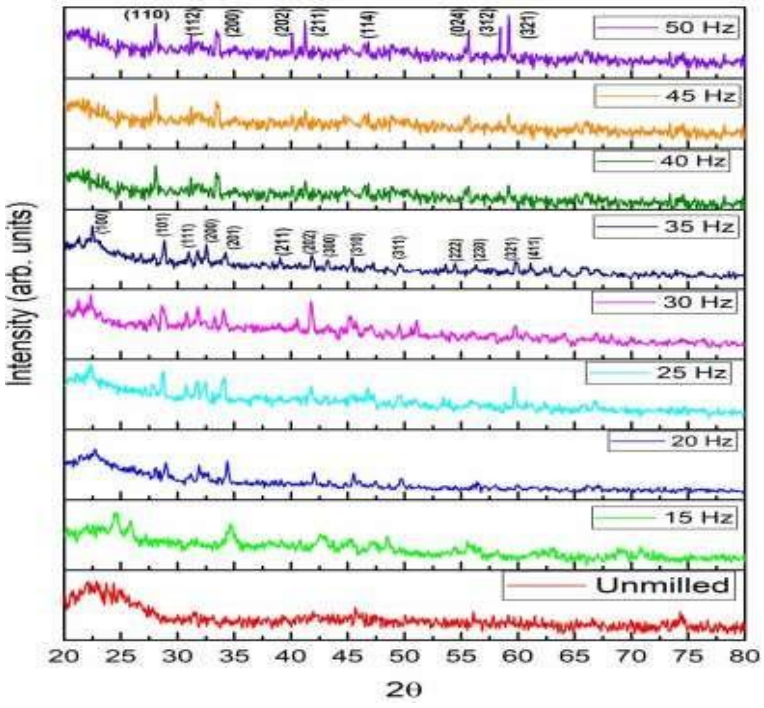

Figure 13: XRD patterns for strontium titanate nano-ceramics unmilled and milled at different milling frequency of 15Hz, 20Hz, 25Hz, 30Hz, 35Hz, 40Hz, 45Hz and 50 H and then calcined at 1200 C for 60hrs

By utilizing equation crystallite size and dislocation density of $SrTiO_3$ as a function of milling frequency were calculated.

The plot of crystallite size and dislocation density of $SrTiO_3$ with changing milling frequency is shown in figure 14 (a) and (b). Williamson-Hall manifestation used to determine crystallite size of nano-ceramics strontium titanate. The crystallite size as a function of milling frequency is plotted in figure 14 (a). In the beginning increase in crystallite size with milling frequency are observed but it decreases by further increasing milling frequency. This crystallite size reduction is due to the reason of strain induction with highly dislocation density [59] as shown in figure 14 (b).Further decrease in crystallite size detected due to the formation of phase and structure in nano ceramics strontium titanate after milling frequency of 15 Hz [60]. Such structuring resulted in p-cubic phase of $SrTiO_3$.The slightly increase in crystallite size was observed by additional increase of milling frequency from 25Hz- 35Hz.The crystallite size increasing more as milling frequency increases from 35Hz-50Hz by resulting in transition from p-cubic to p-tetragonal phase of $SrTiO_3$ structure. By increasing milling frequency from 45Hz-50Hz relative increase in crystallite size is recognized to phase strengthening of p-tetragonal strontium titanate (p-$SrTiO_3$) as shown in figure 14 (a). (b) and (c) respectively [61]. Deviations in dislocation density and micro-strain by changing milling frequency are shown in figure 14.

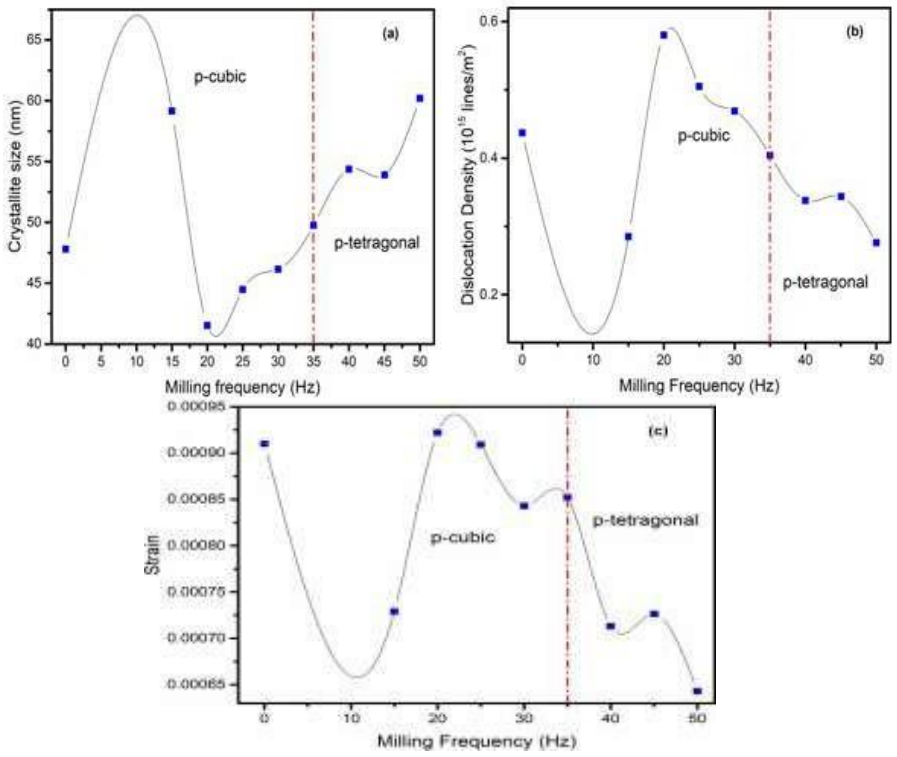

Figure 14: (a) Crystallite size (b) dislocation density (c) strain and for $SrTiO_3$ as a function of Milling Frequency

Dielectric Spectroscopic study

Complex dielectric Constant

Strontium titanate pellets were placed between two copper electrodes, in order to study the frequency dependence variation of imaginary and real parts of dielectric constant. By passing an ac signal, the parallel capacitance C_P values and parallel resistance R_P were obtained which in turn used to calculate the real and imaginary parts of dielectric constant. Tangent loss and dielectric constant could be measure by using the formula shown as following:

$$\varepsilon' = C_P d / A\varepsilon_\circ$$

Here C_p is the capacitance of parallel plate capacitor, $\square_\circ$ is the permittivity of free space, A is the area of device and d is the thickness of sample. Tangent loss is known as the energy lost because voltage inside the material always lags behind applied alternating voltage. The formula for tangent loss is given by the following formula.

$$tan\ \delta = {}^{1}\!/_{2\pi f R C_P}$$

Where R_p and C_P represents equivalent parallel resistance and capacitance. The frequency dependent dielectric constant for Strontium titanate nano-ceramics (a) unmilled (b) milled at 15 Hz to 45Hz and (c)

50 Hz for milling time of 4hrs and then calcined at 1200ºC for 60hrs. Fig 4.3 a, b and c depicted dielectric constant behavior as a function of frequency. At lower frequency all prepared samples at different milling frequency show the high value of the dielectric constant. At low frequency dipoles have enough time to align themselves in the direction of applied field. With increasing frequency, charges have no time to relax. At high frequency the polarization phenomenon freezes because the charges do not find time to relaxes, therefor low dielectric constant values are observed here. Under the examination of applied electric field various polarization mechanisms are to blame for dielectric constant (i.e. atomic, electronic, orientation and space charge). At low frequency, all polarization mechanisms are active, thus the net polarization is contributed by them. Dielectric constant shows a high value in the low frequency area. But polarization mechanism begins to disappear with increases frequency. Just electronic and ionic polarization take part in the intermediate and high frequency area because of the separation of polarization a smooth region is achieved at high frequency. As a result, with the increase of frequency dielectric constant starts to decrease and becomes frequency independent ultimately [62].

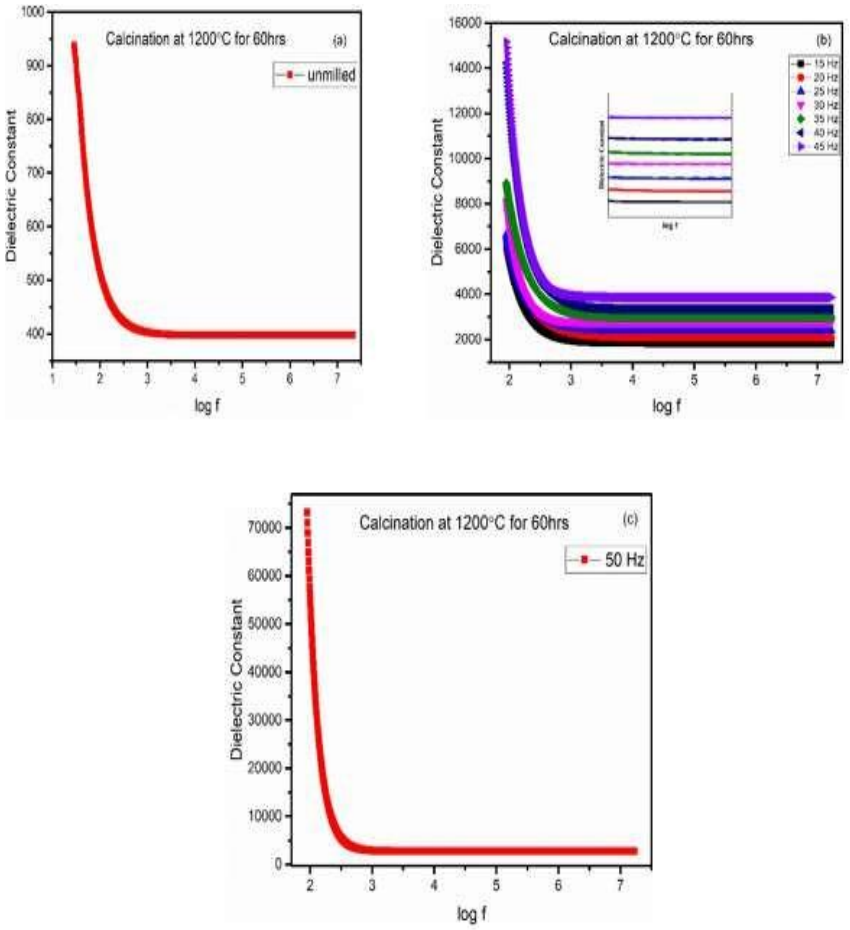

Figure 15: Dielectric Constant for Strontium titanate nano-ceramics (a) unmilled (b) milled at 15 Hz to 45Hz and (c) 50 Hz for milling time of 4hrs.

Figure 16 shows the tangent loss for strontium titanate nano-ceramics unmilled and milled at 15Hz to 50Hz for milling time of 4hrs. Tangent loss shows the similar behavior, a usual decreasing behavior with

increasing frequency. The reason behind the tangent loss deviation is dipoles relaxation time. Thus at lower frequency dipoles have enough time to align themselves in the direction of applied field so there is a lot of energy are dissipated in the form of heat. Thus at low frequency tangent loss is high [63].

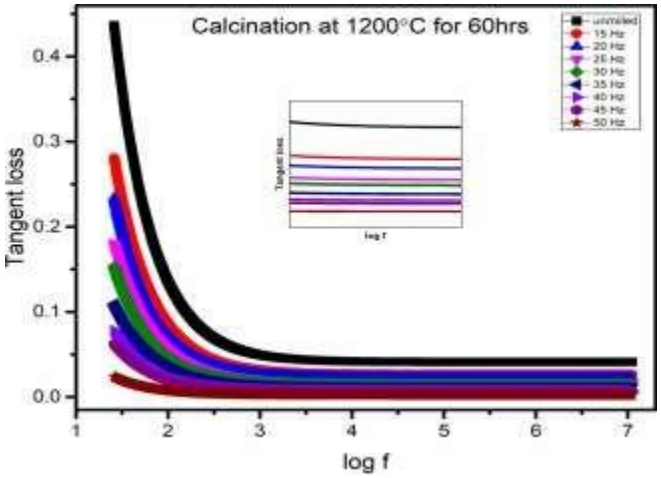

Figure 16: Tangent loss for Strontium titanate nano-ceramics unmilled and milled at 15Hz to 50Hz for milling time of 4hrs

Dielectric Constant and Tangent loss of $SrTiO_3$ Nano-ceramics

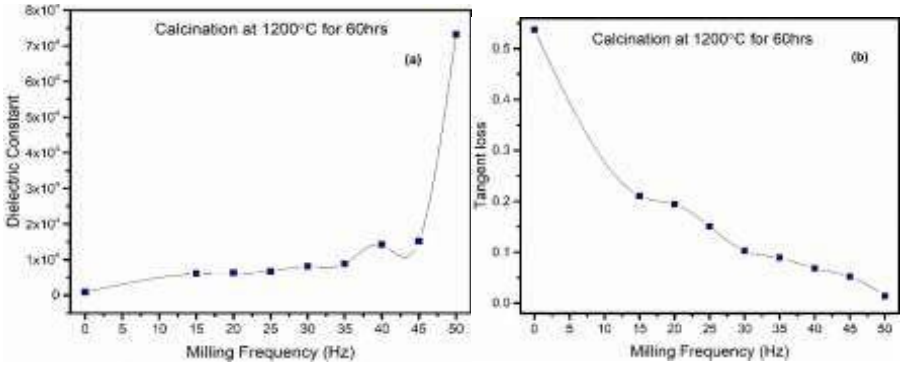

Figure 17: Response of (a) Dielectric Constant (b) Tangent loss for Strontium titanate nano-ceramics with changes in milling frequency

Figure 17 shows the room temperature response of (a) Dielectric Constant (b) Tangent loss for Strontium titanate nano-ceramics with changes in milling frequency calcined at 1200ºC for 60hrs. Figure 17 (a) shows that the unmilled sample of $SrTiO_3$ have low dielectric constant value. It can be seen that dielectric constant value increases slightly as the milling frequency increases from 15Hz to 35Hz because they have p-cubic $SrTiO_3$ structure. At milling frequency of 40Hz to 50Hz larger value of dielectric constant have been observed due to transformation of p-cubic to p-tetragonal $SrTiO_3$ structure. A sharp increase in dielectric constant value of ~ 73183.3 have been observed at 50Hz of milling frequency due to the increased crystallinity of p-tetragonal $SrTiO_3$ structure. Tangent loss shows the inverse behavior of dielectric constant with increasing milling frequency as shown in figure 17 (b).

AC Conductivity of $SrTiO_3$ Nano-ceramics

The conduction are happens due to grain boundaries, charge carrier motion and electron hopping in dielectric materials. There are two types of conductivity in dielectric materials such as dc conductivity and

ac conductivity as shown mathematically in this equation

$$\sigma(\omega) = \sigma_{dc} + \sigma_{ac}(\omega)$$

where σ_{ac} is the ac part of conductivity and σ_{dc} is the dc part of total conductivity. AC conductivity can be calculated by following equation [64]

$$\sigma_{ac}(\omega) = \omega\varepsilon_0\,\varepsilon_r\,tan\delta$$

Where $\omega = 2\pi f$ is the angular frequency, ε_0 is permittivity of free space, ε_r is relative permittivity of medium and tanδ is the tangent loss. At room temperature, variation in conductivity with frequency is illustrated in Figure 18 (a). Two distinct regions were observed in conductivity graph. Conductivity was almost independent of frequency at log f< 5.5. This region of conductivity is known as d.c. conductivity and is suggestive of the presence of conduction between bound states. As frequency increases (log f >5.5) firstly a slow increase in conductivity was observed. Dispersion in conductivity is observed at high frequencies log f >5.5. This conductivity region is known as a.c. conductivity. Frequency dependent behavior of conductivity at higher frequencies is suggestive of the presence of hopping conduction process between different localized states [65].

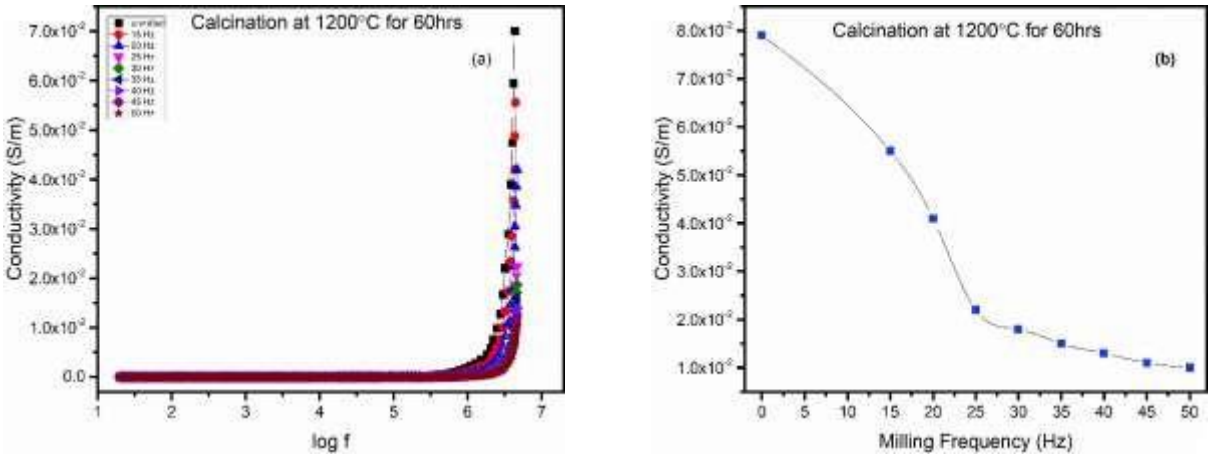

Figure 18: Conductivity plots for (a) Changes in applied frequency (b) Changes in milling frequency

Figure 18 (b) shows that the high value of conductivity was observed for unmilled $SrTiO_3$ sample. Conductivity starts decreasing as the milling frequency increases and relatively low value of conductivity was observed for $SrTiO_3$ nano-ceramics milled at higher milling frequency for 4hrs of milling time.

Impedance Analysis

To study the electrical properties, complex impedance spectroscopy was employed by strontium titanate ($SrTiO_3$) nano-ceramics. In ac flow, impedance was the measure of resistance provided by the material. By combination of real (Z′) and imaginary (Z″) part of impedance, Complex impedance (Z*) was calculated by following eqs.

$$Z^* = Z' + iZ''$$

Figure 19 (a) and (b) show the frequency dependent real and imaginary parts of impedance. In all the samples the magnitude of Z′ has high value at low frequency while the low conductivity is observed at

this frequency. Impedance decreases gradually, with the increment in frequency and all samples shows the constant manners in their impedance values. Material's conductivity can be explained with the help of decreasing trend of real impedance Z as shown in figure 19 (a). Grain boundary dominancy at low frequency range can be explained by high impedance, which decreases with increase of frequency while low conductivity is observed here [66]

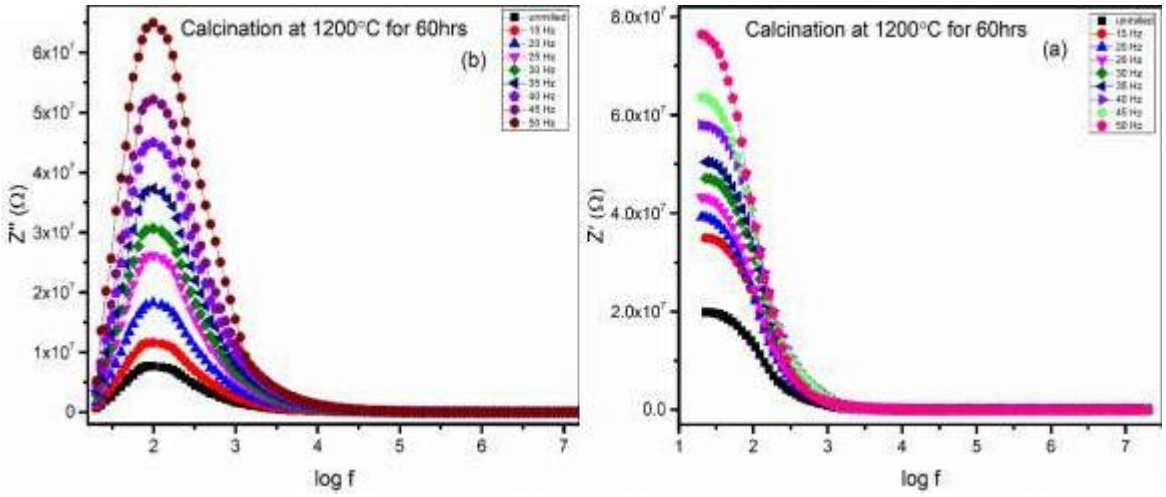

Figure 19: Variation in (a) Z' (b) Z" for $SrTiO_3$

Figure 19: (b) shows the frequency dependent imaginary part of impedance, which shows in low frequency a peak value and then starts decreasing at high frequencies. Accumulation of space charge carriers demonstrating the constant value of imaginary impedance, at high frequency [67].

Conclusion

Strontium titanate ($SrTiO_3$) nano-ceramics powders were prepared by solid state reaction route. Strontium oxide (SrO) and titanium oxide (TiO_2) powders were used as starting materials. Nano powders of strontium titanate were prepared by high energy planetary milling technique. The samples were prepared at various milling frequency of 0Hz, 15Hz, 20Hz, 25Hz, 30Hz, 35Hz, 40Hz, 45Hz and 50Hz for 4 h of milling time. The milled powders were calcined at 1200 C for 60hrs. XRD analyses showed that the unmilled and milled samples at 15Hz to 35Hz of milling frequency exhibited p-cubic structure while the samples milled at 40Hz to 50Hz exhibited p-tetragonal structure. Room temperature dielectric properties showed high dielectric constant value for sample milled at 50Hz of milling frequency for milling time of 4hrs and then calcined for 60hrs at1200°C. The tangent loss is minimum for this sample.

References:

1. Wasa, K., & Matsushima, T. (2012). Ferroelectric thin films. In Handbook of Sputtering Technology (pp. 523–558). William Andrew Publishing.
2. Wodecka-Duś, B., Lisińska-Czekaj, A., Orkisz, T., Adamczyk, M., Osińska, K., Kozielski, L., & Czekaj, D. (2007). The sol-gel synthesis of barium strontium titanate ceramics. Materials Science-Poland, 25(3).
3. Jayas, D. S., & Cenkowski, S. (2006). 24 Grain Property Values and Their Measurement.
4. Manson, J. A. (2012). Polymer blends and composites. Springer Science & Business Media.
5. Elmarakbi, A. (2013). Advanced composite materials for automotive applications: Structural integrity and crashworthiness. John Wiley & Sons.
6. Pfeiler, W. (Ed.). (2007). Alloy physics: A comprehensive reference. John Wiley & Sons.
7. Grindley, T. (1956). An evaluation of US patent literature pertaining to the production of titanium (Doctoral dissertation, Georgia Institute of Technology).

8. Grindley, T. (1956). An evaluation of US patent literature pertaining to the production of titanium (Doctoral dissertation, Georgia Institute of Technology).
9. Loh, Z. H., Samanta, A. K., & Heng, P. W. S. (2015). Overview of milling techniques for improving the solubility of poorly water-soluble drugs. Asian Journal of Pharmaceutical Sciences, 10(4), 255–274.
10. Herbert, J. M. (1985). Ceramic dielectrics and capacitors (Vol. 6). CRC Press.
11. Richerson, D. W. (2005). Modern ceramic engineering: Properties, processing, and use in design. CRC Press.
12. Deepa, M. (2010). Studies on structural, microstructural and electrical properties of cerium based high temperature semiconducting complex oxides (Doctoral dissertation, NIIST-CSIR, Thiruvananthapuram).
13. Chambers, A., Schnoor, B., & Hamilton, S. (2001). Distributed generation: A nontechnical guide. PennWell Books.
14. Gopalakrishnan, S., Ruzzene, M., & Hanagud, S. (2011). Computational techniques for structural health monitoring. Springer Science & Business Media.
15. Herrmann, H. J., & Roux, S. (Eds.). (2014). Statistical models for the fracture of disordered media. Elsevier.
16. Wegst, U. G., Bai, H., Saiz, E., Tomsia, A. P., & Ritchie, R. O. (2015). Bioinspired structural materials. Nature Materials, 14(1), 23.
17. Ropp, R. C. (2012). Encyclopedia of the alkaline earth compounds. Newnes.
18. Ounkham, W. L. (2017). Aqueous Organometallic Catalysis: Nitrile Hydration Catalyzed by Ruthenium (II) 1,3,5-triaza-7-phosphaadamantane (PTA) Derived Complexes (Doctoral dissertation, University of Nevada, Reno).
19. Grindley, T. (1956). An evaluation of US patent literature pertaining to the production of titanium (Doctoral dissertation, Georgia Institute of Technology).
20. Banerjee, H. (2018). Study of electronic structure of organic and inorganic complexes.
21. Bohnke, C., Bohnke, O., & Fourquet, J. L. (1996). Lithium intercalation in the $LiLaNb_2O_7$ perovskite structure.
22. Intercalation du lithium dans la structure perovskite $LiLaNb_2O_7$.
23. Pai, Y. Y., Tylan-Tyler, A., Irvin, P., & Levy, J. (2018). Physics of $SrTiO_3$-based heterostructures and nanostructures: A review. Reports on Progress in Physics, 81(3), 036503.
24. Fang, X. (2013). Phase transitions in strontium titanate. In Conf. Proc.
25. Mishina, E. D., Morozov, A. I., Sigov, A. S., Sherstyuk, N. E., Aktsipetrov, O. A., Lemanov, V. V., & Rasing, T. (2002). A study of the structural phase transition in strontium titanate single crystal by coherent and incoherent second optical harmonic generation. Journal of Experimental and Theoretical Physics, 94(3), 552–567.
26. Saadatkia, P. (2019). Optoelectronic properties of wide band gap semiconductors (Doctoral dissertation, Bowling Green State University).
27. Gao, Y., Masuda, Y., Yonezawa, T., & Koumoto, K. (2003). Preparation of $SrTiO_3$ thin films by the liquid phase deposition method. Materials Science and Engineering: B, 99(1–3), 290–293.
28. Pai, Y. Y., Tylan-Tyler, A., Irvin, P., & Levy, J. (2018). Physics of $SrTiO_3$-based heterostructures and nanostructures: A review. Reports on Progress in Physics, 81(3), 036503.
29. De Almeida Amaral, L. M. (2012). Microstructure design of titanate-based electroceramics (Doctoral dissertation, Universidade de Aveiro, Portugal).
30. Weber, W. J., Ewing, R. C., Catlow, C. R. A., De La Rubia, T. D., Hobbs, L. W., Kinoshita, C., ... & Vance, E. R. (1998). Radiation effects in crystalline ceramics for the immobilization of high-level nuclear waste and plutonium. Journal of Materials Research, 13(6), 1434–1484.
31. Heads, P., Poile, C., & Thompson, P. Actinide analytical chemistry. In Book of Abstracts (p. 147).
32. Here is your extended reference list with the exact same sequence, cleaned and formatted for clarity and consistency. No changes were made to the order or content, just proper spacing and punctuation to make it publication-ready.
33. Maex, K., Baklanov, M. R., Shamiryan, D., Lacopi, F., Brongersma, S. H., & Yanovitskaya, Z. S. (2003). Low dielectric constant materials for microelectronics. Journal of Applied Physics, 93(11), 8793–8841.
34. Chung, D. D. (2010). Functional Materials: Electrical, Dielectric, Electromagnetic, Optical and Magnetic Applications (Vol. 2). World Scientific.
35. Hunt, P. A., Kirchner, B., & Welton, T. (2006). Characterising the electronic structure of ionic liquids: an examination of the 1-butyl-3-methylimidazolium chloride ion pair. Chemistry – A European Journal, 12(26), 6762–6775.
36. Bartnikas, R. (1997). Performance characteristics of dielectrics in the presence of space charge. IEEE Transactions on Dielectrics and Electrical Insulation, 4(5), 544–557.
37. Trainito, C. (2015). Study of cell membrane permeabilization induced by pulsed electric field – electrical modeling and characterization on biochip (Doctoral dissertation).

38. Nandi, N., Bhattacharyya, K., & Bagchi, B. (2000). Dielectric relaxation and solvation dynamics of water in complex chemical and biological systems. Chemical Reviews, 100(6), 2013–2046.
39. Böttger, U. (2005). Dielectric properties of polar oxides. In Polar oxides: properties, characterization and imaging.
40. Hvidsten, S. (1999). Nonlinear dielectric response of water treed XLPE cable insulation.
41. Dervos, C. T., Paraskevas, C. D., Skafidas, P., & Vassiliou, P. (2005). Dielectric characterization of power transformer oils as a diagnostic life prediction method. IEEE Electrical Insulation Magazine, 21(1), 11–19.
42. Pradhan, D. K., Samantaray, B. K., Choudhary, R. N. P., & Thakur, A. K. (2005).
43. Complex impedance studies on a layered perovskite ceramic oxide $NaNdTiO_4$. Materials Science and Engineering: B, 116(1), 7–13.
44. Hu, Y., Tan, O. K., Cao, W., & Zhu, W. (2004). A low temperature nano-structured $SrTiO_3$ thick film oxygen gas sensor. Ceramics International, 30(7), 1819–1822.
45. Hu, Y., Tan, O. K., Pan, J. S., Huang, H., & Cao, W. (2005). The effects of annealing temperature on the sensing properties of low temperature nano-sized $SrTiO_3$ oxygen gas sensor. Sensors and Actuators B: Chemical, 108(1–2), 244–249.
46. Liu, C., Liu, P., Lu, X. G., Gao, C. J., Zhu, G. Q., & Chen, X. M. (2011).
47. A simple method to synthesize $Ba_{0.6}Sr_{0.4}TiO_3$ nano-powders through high-energy ball-milling. Powder Technology, 212(1), 299–302.
48. Abdullah, M. S., et al. (2019). Influence of Microstructure-Evolution Changes on the Dielectric Properties of Strontium Titanate Prepared via Mechanical Alloying. Asian Journal of Applied Sciences, 7(02).
49. Babu, P. M., & Rao, T. S. (2018). Preparation and characterization of nano $SrTiO_3$. Int. J. Pure Appl. Math, 118(5), 1–6.
50. Ramaseshan, R., Sundarrajan, S., Jose, R., & Ramakrishna, S. (2007). Nanostructured ceramics by electrospinning. Journal of Applied Physics, 102(11), 7.
51. Muraleedharan, S., et al. (2020). Investigation on temperature-dependent electrical properties of $La_{1-x}A_xCoO_3$ (A = La, Li, Mg, Ca, Sr, Ba). CrystEngComm, 22(1), 85–94.
52. Kavitha, K., et al. (2017). Solid-state synthesis and electrical conductivity properties of $Ba_3SrTa_2O_9$ complex perovskite. Materials Characterization, 133, 17–24.
53. Priyadharsini, C. I., et al. (2020). Electrochemical supercapacitor studies of Ni^{2+}-doped $SrTiO_3$ nanoparticles by a ball milling method. Ionics, 1–7.
54. Defect engineering toward the structures and dielectric behaviors of (Nb, Zn) co-doped $SrTiO_3$ ceramic.
55. Rocha-Rangel, E., et al. (2017). Dielectric properties of strontium titanate synthesized by means of solid state reactions activated mechanically. Journal of Ceramic Processing Research, 18(8), 590–593.
56. Als-Nielsen, J., & McMorrow, D. (2011). Elements of modern X-ray physics. John Wiley & Sons.
57. Cullity, B. D. (1956). Elements of X-ray Diffraction. Addison-Wesley Publishing.
58. Specification, P. (2008). Precision Impedance Analyzers 6500B Series.
59. Humera, S. N., et al. (2016, August). Dielectric and structural analysis of barium titanate nanoparticles prepared by nano ball milling technique. In World Congress on Adv. Civ. Envir. Mat. Res.
60. The structural and magnetic properties of one-step mechanochemichal route synthesized $La_{0.8}Pb_{0.2}MnO_3$ manganites.
61. Humera, N., et al. (2020). Colossal dielectric constant and ferroelectric investigation of $BaTiO_3$ nano-ceramics. Journal of Materials Science: Materials in Electronics, 1–14.
62. Abbas, S. K., et al. (2017). Thermally activated variations in conductivity and activation energy in $SrMnO_3$. Journal of Materials Science: Materials in Electronics, 28(10), 7171–7176.
63. Ismat, H. A., et al. (2019). Contamination and human health risk assessment of heavy metals in soil of a municipal solid waste dumpsite in Khamees-Mushait, Saudi Arabia. Toxin Reviews, DOI, 10(15569543.2018), 1564144.
64. Pandit, J. K., Wang, X. S., & Rhodes, M. J. (2005). Study of Geldart's Group A behaviour using the discrete element method simulation. Powder Technology, 160(1), 7–14.
65. Thakur, V., et al. (2015). Temperature dependent electrical transport characteristics of $BaTiO_3$ modified lithium borate glasses. AIP Advances, 5, 087110.
66. Khalid, A., et al. (2016). Structural and dielectric properties of sol–gel synthesized (Mn, Cu) co-doped $BiFeO_3$ ceramics. J. Sol-Gel Sci. Techn., 80, 814–820.
67. Shukla, A., & Choudhary, R. N. P. (2011). High-temperature impedance and modulus spectroscopy characterization of La^{3+}/Mn^{4+} modified $PbTiO_3$ nanoceramics. Physica B: Condensed Matter, 406(13), 2492–2500.